

# STUDIES OF RESISTIVE WALL HEATING AT JLAB FEL

R. Li and S. Benson, Jefferson Lab, Newport News, VA23693, USA

## Abstract

Temperature rise over the wiggler vacuum chamber was observed when the JLAB FEL is under CW operation during IR upgrade. As an effort to understand the observed phenomena, in this study we estimate the resistive wall induced power loss using existing theories for various cases, such as DC and AC conductivity. We also estimate the non-ultrarelativistic effect on resistive wall loss for pipe with both round cross section and parallel plates. In this paper we present the comparison of our results with the measured data obtained during CW operation of the JLAB FEL. Other factors possibly contributing to the measured heating will also be discussed.

## INTRODUCTION

The resistive wall effect induced wall heating can cause significant problems for high power operation of accelerators involving narrow waveguide gap. During the early stage of high power operation of JLAB IR upgrade, wall heating is observed and measured for the wiggler chamber (with 100 mm  $\times$  12 mm rectangular cross section) [1]. With the CW electron beam and 150 fs rms bunch length, the resistive wall heating at JLAB FEL provides a unique opportunity to study the resistive wall effect in the regime of both high peak current and high average current. Understanding the measurement of wall heating at Jefferson Lab is important for scale-up designs of future higher power FELs. Resistive wall effect also plays a critical role in the design of undulators with minimum period (and thus gap size) acceptable by the resistive wall impedance in the effort to push the short-wavelength front of FEL designs with minimum possible linac cost [2].

The resistive wall effect for JLAB FEL wiggler chamber is in the regime of flat geometry for non-ultrarelativistic beams. To see how the geometry and ultrarelativity properties contribute to the observed phenomena, we first estimate the resistive wall induced beam energy loss using existing theories for JLAB parameters. This includes both DC and AC effects for a cylindrical waveguide in both the ultra-relativistic limit and the non-ultrarelativistic cases [3-5]. We will then estimate the non-relativistic effect for a parallel plate geometry using a recently developed theory [6], and will comment on the anomalous skin effect. Our results are compared with the measured data obtained during CW operation of the JLAB FEL. Other possible factors contributing to the measured heating will also be discussed.

## OBSERVATION OF WALL HEATING

During the attempt of high power operation of the JLAB IR upgrade using CW electron beams, it is found [1] that as the bunch current gets higher, the laser power drops as the result of mirror displacement due to heat expansion of the wiggler chamber. To characterize the observed wall heating, copper plates were attached to the chamber wall and the plates were water cooled. The power deposited on the chamber wall can be calculated by measuring the water running rate and temperature rise of the water. Measurements show that for stainless steel pipe, at  $I = 3.5$  mA, the power deposited to the wall is 32 W/mA/m (meaning per unit meter of undulator length). For a pipe with 1.3  $\mu\text{m}$  thick sputtered copper coating, at  $I = 2.5$  mA, the power deposited to the wall is 12 W/mA/m. It is also found that the rise of water temperature depends both on the beam current and bunch length. For convenience, we list the observation in Table 1.

Table 1: Observed Power Deposit

Waveguide Wall Material	Power Deposit on Wiggler Chamber
Stainless Steel	32 W/mA/m
Copper Coated	12 W/mA/m

This observation motivates us to investigate the possible contribution from the resistive wall effect, which can be significant when the high average current beam traversing through the narrow wiggler chamber.

## ESTIMATION USING EXISTING THEORIES

As the first attempt to explain the measured wall heating at JLAB FEL, we estimate the resistive wall induced beam power loss predicted by the existing theories. Since there was no dedicated effort of beam characterization when wall heating was measured, in this study the estimations are carried out for a generic set of JLAB FEL parameters as listed in Table 2, assuming an ideal Gaussian longitudinal bunch distribution. The discussion on the effect of high frequency component in a realistic bunch distribution will be followed.

Table 2: Generic Parameters

Average current	$I_{\text{ave}}$	4 mA
Bunch rms size	$\sigma_z$	45 $\mu\text{m}$
Beam energy	$E$	135 MeV
Bunch charge	$Q_b$	110 pC
Gap size	$b$	6 mm

*Cylindrical Pipe with DC Conductivity ( $v=c$ )*

The impedance for a cylindrical resistive waveguide [3] with DC conductivity (for  $\omega = kc$ ) is

$$Z_{||}(\omega) = \frac{Z_0}{2\pi b} \frac{1}{\lambda/k - ikb/2}, \quad (1)$$

which represents a broad-band resonance with the characteristic length of

$$s_0 = \left( \frac{cb^2}{2\pi\sigma} \right)^{1/3}$$

for the conductivity  $\sigma$  and  $\lambda^2 = 4\pi\sigma ik/c$ . For parameters in Table 1,  $s_0 = 15 \mu\text{m}$  for copper coated chamber and  $s_0 = 51 \mu\text{m}$  for stainless steel case. Note that the JLAB FEL parameters are such that for stainless steel case  $s_0 = 1.1 \sigma_z$ . The bunch spectrum lies in the region  $k\sigma_z \sim 1$ , hence it samples the resonance peak of the resistive wall impedance as shown in Fig. 1, causing more resistive wall loss than that in the copper coated case. The resulting power loss is listed in Table 3, as calculated by

$$\frac{dP}{dL} = \frac{I_{\text{ave}} Q_b c}{\pi} \int_0^\infty dk |f(k)|^2 \text{Re}(Z(k)), \quad (2)$$

with  $f(k)$  the bunch frequency component. Note that the estimation for Table 3 assumes an Gaussian bunch.

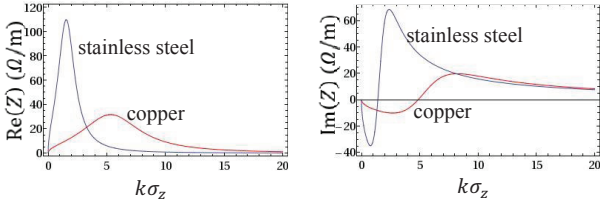


Figure 1: DC Impedance at  $r = 6 \text{ mm}$  for  $v = c$ .

*Cylindrical Pipe with AC Conductivity ( $v=c$ )*

For a copper pipe, the relaxation time  $c\tau = 8.1 \mu\text{m}$ . We need to replace the DC conductivity in Eq. (1) by the AC conductivity  $\bar{\sigma} = \sigma/(1 - i\omega\tau)$ . The impedance is shown in Fig. 2, with the green curve representing the Gaussian bunch spectrum. Even though the AC impedance peaked at higher amplitude, the bunch spectrum is substantial only at lower frequency and does not sample the impedance resonance. The beam power loss for the AC case is listed in Table 3. The relaxation time for stainless steel is not available. In this estimation we assume the same relaxation time for stainless steel as that for copper.

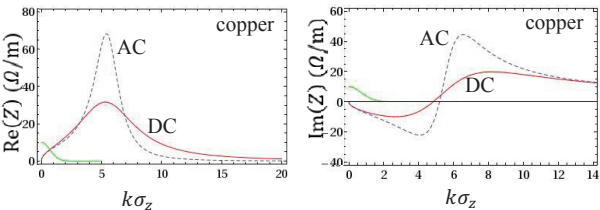


Figure 2: DC and AC impedance at  $r = 6 \text{ mm}$ . The green curve is the bunch frequency spectrum.

Table 3: Cylindrical Pipe ( $v = c$ )

Wall Material	Power Loss (DC)	PowerLoss (AC)
Stainless Steel	16.5 W/mA/m	20.5 W/mA/m
Copper Coated	1.9 W/mA/m	1.8 W/mA/m

*Cylindrical Pipe with DC Conductivity ( $v < c$ )*

For ultrarelativistic case when  $v = c$ , the electric field lines from a source electron moving in free space are Lorentz contracted into a 2D pancake. When  $v < c$ , the pancake opens an angle  $\theta \sim 1/\gamma$ , as illustrated in Fig. 3. For  $k \sim \sigma_z^{-1}$ ,  $E = 135 \text{ MeV}$ , we have  $kb/\gamma \sim 0.5$  for parameters in Table 1. The spread of the pancake on the wall is now half the bunch length, causing smearing effect and reduction of resistive wall impedance at high frequency.

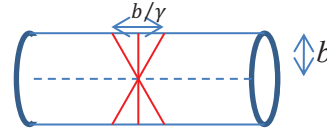


Figure 3: Field line spread in  $v < c$  case.

The effect of non-ultrarelativity on a cylindrical resistive wall is fully analysed [4], and simplified as [5]

$$Z_{||}(\omega) = \frac{Z_0}{2\pi b} \frac{s_0}{b} \left[ (I_0(k_r b))^2 P(k) \right]^{-1} \quad (3)$$

for  $k_r = k/(\gamma\beta)$ , with  $P(k) = -i \frac{I_1(k_r b)}{I_0(k_r b)} + \frac{(1+i)b}{\gamma\beta k^{1/2} s_0^{3/2}}$ .

For a copper coated pipe, the comparison of  $\text{Re}(Z)$  for ultrarelativistic case and non-ultrarelativistic case is shown in Fig. 4. We can see that non-ultrarelativity causes a big reduction in the amplitude of impedance resonance. However, the low frequency part of the impedance is less impacted. For the copper case, since the bunch frequency is much lower than the resonance frequency, or  $s_0 = \sigma_z/3$ , the bunch power loss is reduced only by 15% from the non-ultrarelativistic effect.

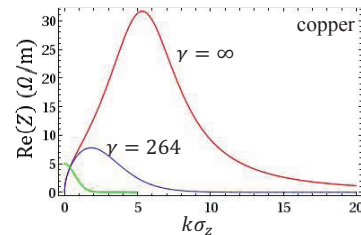


Figure 4: DC Impedance for  $r = 6 \text{ mm}$  at  $E = 135 \text{ MeV}$ . The green curve is the bunch frequency spectrum.

## PARALLEL PLATE WITH NON-ULTRARELATIVISTIC EFFECT

For ultrarelativistic case, the analyses of resistive wall impedance was previously extended [7] from circular cross section to rectangular cross section. To account for the resistive wall induced heating effect at JLAB FEL, we need to extend the previous theory to the regime of non-ultrarelativistic effect on resistive wall impedance for a flat geometry. In this section, we summarize our recent theoretical impedance study for  $v < c$  case with resistive parallel plate boundary conditions. The impedance results will be compared with the previous results obtained for  $v = c$  case.

For a flat geometrical boundary condition, the cylindrical symmetry of the source field breaks. As a result, both TE and TM modes exist for the homogeneous solution of the fields. In addition, the non-ultrarelativistic effect introduces additional space charge fields in flat geometry, so one expects that the factor  $kb/\gamma$  will play an important role in impedance reduction when  $v < c$ . An analysis on resistive wall impedance for parallel plates in non-ultrarelativistic regime is carried out recently [6], and the finding is that for  $\omega = k/v$  and  $\alpha^2 = \eta^2 + k^2/\gamma^2$ ,

$$Z_{\parallel}(\omega) = \frac{Z_0 \beta^2}{4\pi} Q(k) \quad (4)$$

for

$$Q(k) = \int_{-\infty}^{\infty} \frac{d\eta}{\frac{\lambda}{k} (\cosh(\alpha b))^2 - \frac{ik}{\alpha} \cosh(\alpha b) \sinh(\alpha b)}.$$

At ultrarelativistic limit,  $\gamma \rightarrow \infty$ , the above expression will be reduced to the previous results [8]

$$Z_{\parallel}(\omega) = \frac{Z_0}{4\pi} Q_0(k) \quad (5)$$

for

$$Q_0(k) = \int_{-\infty}^{\infty} \frac{d\eta}{\frac{\lambda}{k} (\cosh(\eta b))^2 - \frac{ik}{\eta} \cosh(\eta b) \sinh(\eta b)}.$$

The comparison of impedances in Eqs. (1), (4), and (5) are shown in Fig. 5.

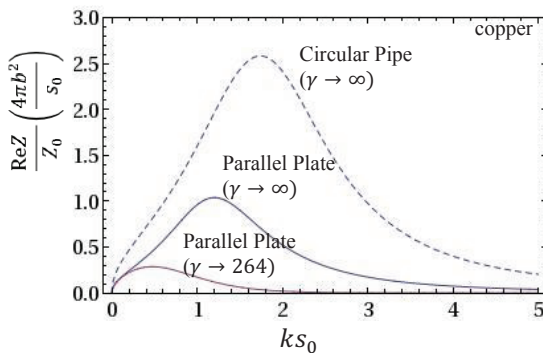


Figure 5: Geometric and non-ultrarelativistic effect on impedance for  $b = 6$  mm at  $E = 135$  MeV.

We can see that for  $v = c$ , when the chamber cross section changes from circle to parallel plate, there is a significant reduction of amplitude of the real part of resistive wall impedance. The non-ultrarelativistic effect will further reduce amplitude from that for the ultrarelativistic case. The method employed for this analysis can be straightforwardly extended to the study of transverse dipole resistive wall impedance and wake-fields.

## DISCUSSIONS

The parameters of resistive wall heating in the JLAB FEL wiggler chamber lie in an interesting regime that each of the following features needs to be carefully evaluated: high characteristic bunch frequency close to the resistive wall resonance frequency, AC conductivity, non-ultrarelativistic beams and flat geometry. Our estimations in Table 3, assuming beam with ideal Gaussian bunches, can explain 50% of the observed power deposit for stainless steel wall and 15% for copper wall. Considerations of flat geometry and non-ultrarelativistic effect lead to further reduction for the power loss estimations. Possible causes of higher observed power deposit are (1) the high frequency bunch structure in realistic beams and (2) the possible effect of surface roughness combined with wall resistivity. From the impedance behaviour in Figs. 1, 2 and 4, 5, one can foresee that higher frequency components in  $f(k)$  of Eq. (2) can result in more beam power loss to the resistive wall. So it is important to have a systematic measurement of the resistive wall heating along with careful bunch characterization. For a copper coated chamber, it is interesting to compare the skin depth  $\delta_{\text{skin}} \approx 63$  nm with the coating thickness  $d$ , and also to check the anomalous skin effect by comparing  $\delta_{\text{skin}}$  with the mean free path  $l$ . For  $\omega \approx c/\sigma_z$ , we have  $\delta_{\text{skin}} \approx 63$  nm, which is well below the thickness of  $d = 1.3 \mu\text{m}$  used in the JLAB wiggler chamber. We also note that at room temperature, the mean free path  $l = 40$  nm is comparable to  $\delta_{\text{skin}}$ . This is at the borderline when the Ohm's law still holds. However, the anomalous skin effect is usually most prominent at low temperature, and it is negligible at our high frequency regime [9].

## REFERENCES

- [1] S. Benson, JLAB-Technote, 2013.
- [2] R. York, private communication, 2013.
- [3] K. Bane, SLAC/AP-87, 1991.
- [4] F. Zimmermann and K. Oide, PRAT-AB 7, 044201 (2004).
- [5] A. Macridin *et al.*, PRST-AB **14**, 061003 (2011)
- [6] R. Li, to be published (2013).
- [7] H. Henke and O. Napoly, CERN/LEP-RF/89-71 (1989). K. Yokoya, KEK-preprint, 92-196 (1993). K. Y. Ng, FN-0744 (2004)
- [8] K. Bane and G. Stupakov, SLAC-PUB-10707 (2004).
- [9] G.E.H. Reuter and E.H. Sondheimer, *Proc. R. Soc. Lond. A* **195**, 336-364 (1948).